The transcriptional landscape of αβ T cell differentiation

Published in final edited form as:
Nat Immunol. 2013 June ; 14(6): . doi:10.1038/ni.2590.

The transcriptional landscape of αβ T cell differentiation

Michael Mingueneau[1,†], **Taras Kreslavsky**[2,†], **Daniel Gray**[3,†], **Tracy Heng**[4,†], **Richard Cruse**[1], **Jeffrey Ericson**[1], **Sean Bendall**[5], **Matt Spitzer**[5], **Garry Nolan**[5], **Koichi Kobayashi**[2,6], **Harald von Boehmer**[2], **Diane Mathis**[1,*], **Christophe Benoist**[1,*], and **Immunological Genome Consortium**[$]

[1]Division of Immunology, Department of Microbiology and Immunobiology, Harvard Medical School, Boston, MA 02115, USA

[2]Dana-Farber Cancer Institute, Boston, MA, USA

[3]Department of Medical Biology, University of Melbourne, Parkville, VIC 3010, Australia and Molecular Genetics of Cancer Division and Immunology Division, The Walter and Eliza Hall Institute of Medical Research, Parkville, VIC 3052, Australia

[4]Department of Anatomy and Developmental Biology, Monash University, Clayton, VIC 3800, Australia

[5]Stanford University School of Medicine, Palo Alto, CA

[6]Texas A&M Health Science Center, College Station, TX

Abstract

αβT cell differentiation from thymic precursors is a complex process, explored here with the breadth of ImmGen expression datasets, analyzing how differentiation of thymic precursors gives rise to transcriptomes. After surprisingly gradual changes though early T commitment, transit through the $CD4^+CD8^+$ stage involves a shutdown or rare breadth, and correlating tightly with MYC. MHC-driven selection promotes a large-scale transcriptional reactivation. We identify distinct signatures that mark cells destined for positive selection versus apoptotic deletion. Differential expression of surprisingly few genes accompany CD4 or CD8 commitment, a similarity that carries through to peripheral T cells and their activation, revealed by mass cytometry phosphoproteomics. The novel transcripts identified as candidate mediators of key transitions help define the “known unknown” of thymocyte differentiation.

Introduction

The Immunological Genome Project (ImmGen) is an international collaboration of laboratories that collectively perform a thorough dissection of gene expression and its regulation in the immune system of the mouse. Here, we track the transcriptome through the entire differentiation pathway of T cells in the thymus against the backdrop of all ImmGen data, finding unexpectedly gradual changes, sharp breakpoints, and similarities.

[*]Address correspondence to: Christophe Benoist and Diane Mathis, Division of Immunology, Department of Microbiology and Immunobiology, Harvard Medical School, 77 Avenue Louis Pasteur, Boston, MA 02115, cbdm@hms.harvard.edu, Phone: (617) 432-7741, Fax: (617) 432-7744.
[†]Equal contributors
[$]Full list of collaborators appears at back

The authors have no conflicting financial interests.

The vertebrate thymus is where hematopoietic precursors differentiate into T cells. This differentiation process has been intensively studied over several decades [1], resulting in what is arguably the most finely parsed of any differentiation cascade among mammalian cell-types [2-9]. The sequence runs from the commitment of lymphoid precursors to the T cell lineage, random rearrangement of T cell receptor (TCR) genes, and selection that allows maturation of only those thymocytes bearing potentially useful TCR specificities (positive selection) and that do not overreact to self (negative selection). These steps are distinguished by the expression of certain cell surface molecules. The most immature thymocytes lack the expression of the CD4 and CD8 co-receptors (double negative, DN) and can be further subdivided into subsets that track the commitment to become T cells using CD25 and CD44 expression [10], along with c-KIT (reviewed by [11]) and CD28 [12]. Functional rearrangement and expression of a γδTCR promotes proliferation accompanied by early maturation of DN progenitors and subsequent emigration from the thymus [13].

In contrast, successful TCRβ gene rearrangement in the DN subset initiates several rounds of proliferation essential for αβ differentiation and the generation of $CD4^+CD8^+$ double positive (DP) thymocytes [14], where TCRα rearrangement takes place. DP thymocytes screen thymic cortical epithelial cells for the potential of their TCR to interact with peptide-MHC complexes (pMHC) [15-18]. Those DP thymocytes bearing TCR that cannot bind self-pMHC (thought to be the majority) die within three to four days [19]. Those DP thymocytes that express a TCR that can interact with MHC class I or MHC class II molecules are positively selected and correspondingly mature as $CD4^-CD8^+$ single positive (CD8SP) or $CD4^+CD8^-$ (CD4SP) thymocytes (lineage commitment) [20]. This positive selection process differs from β-selection, as it occurs in absence of extensive proliferation. If the affinity of the TCR-pMHC interaction is too high, thymocytes are eliminated by apoptosis (clonal deletion), or diverted into alternative lineages such as CD8αα T cells or $FOXP3^+$ regulatory T (Treg) cells [21, 22]. Thymocytes that survive these processes are exported from the thymus and undergo a phase of post-thymic maturation to become functional $CD4^+$ and $CD8^+$ T cells ([23]).

Several of the molecular mediators required for progression through certain stages of thymocyte differentiation have been defined by genetic approaches. What is lacking is a general perspective of how these and other pathways integrate to direct thymocyte differentiation in an unperturbed system. Although numerous studies have profiled thymocyte transcriptomes [24-33], these focused on only limited transitions or selected checkpoints.

Here, we revisited the entire spectrum of differentiation states in the αβ T cell branch of the lymphoid tree from a transcriptional standpoint, using the breadth of ImmGen datasets. This analysis revealed unexpected aspects of T cell differentiation and identified candidate genes whose coordinate regulation at certain transitions hinted at important functions during thymocyte selection and maturation.

Results

Overall perspective of T cell differentiation

We generated gene expression profiles from every stage of thymocyte maturation from early thymic progenitors (ETP) to the most mature single positive (SP) thymocytes ready for export from the thymus (see Supplementary Table 1 for the complete list of population names, abbreviations, and markers used for cell sorting). Profiles from bone marrow progenitors and peripheral naïve T cells were also included. All datasets were generated in duplicate or triplicate from cells obtained from 6 week-old C57Bl/6 male mice. To validate these data, we first assessed the behavior of over 50 well-characterized genes that mark key

events in thymocyte differentiation, such as *Rag1, Tcra*, or *Tcrg*; the expected expression patterns were observed (Fig. 1a, Supplementary Fig. 1 and data not shown). We used several mathematical tools for multivariate analysis to determine the relationships between populations. Unsupervised hierarchical clustering reproduced the known differentiation sequence with striking accuracy (Fig. 1b), indicating that there were no hidden surprises in the αβ T cell branch of the hematopoietic tree determined over the past three decades, and that transcriptional relationships do evolve linearly along differentiation.

We then used Principal Component Analysis (PCA) to map cell populations in a 3D space (Fig. 1c), which again matched the differentiation sequence, but also grouped stages into distinct pods, such as the tightly-knit group of mature SP cells. PCA of the entire ImmGen dataset brought forth a dominant component (PC1, 73% of variance) which tracked generically with maturation in immune lineages (Fig. 1c and data not shown), reminiscent of the major "differentiation" component observed in multivariate mass cytometry analysis of bone marrow cells [34]. γδT cell maturation proceeded directly from the DN3 precursors, while αβ T cells first 'regressed' along this principal component through the intermediate single positive (ISP) and DP stages. For subsequent analyses, we excluded γδT cells (discussed elsewhere [35]) and the DN4 subset (which incorporates both αβTCR and γδTCR thymocytes).

The magnitude of transcriptional changes throughout differentiation was better visualized by plotting the cumulative Euclidean distance between populations (Fig. 1d) or the number of transcripts induced or repressed at each transition (Fig. 1e). These two metrics identified three main "tectonic shifts": between bone marrow precursors and early thymic progenitors (ETPs); at the transition through DN3a; and (the strongest one) around the DP compartment. Contrary to what had been shown for cells developing in OP9-DL1 cocultures [31], *in vivo* commitment to the T cell lineage at the DN2a to DN2b transition was associated with relatively moderate changes (Fig. 1d-e). Although DP blasts resembled earlier β-selected populations, small DP cells were drastically different. Small DP thymocytes were also very different from $CD69^+$ DP, indicating that TCR signaling in DP thymocytes initiated yet another major transcriptional change. In contrast, the transition from $CD69^+$ to terminal CD4SP or CD8SP involved comparatively minor changes, and $CD4^+$ and $CD8^+$ cells looked extremely similar from this perspective (Fig. 1d-e). Finally, egress from the thymus to the periphery had a very small transcriptional impact. Thus, relationships among the transcriptomes recapitulated the currently accepted developmental progression of thymocyte differentiation, and provided several new insights into the transcriptional basis of key transitions.

Early T cell differentiation

The major landmarks of early T cell differentiation (i.e. loss of B cell potential within the ETP and irreversible commitment to the T cell lineage at the DN2a to DN2b transition) happen in a rather discrete manner [9]. By contrast, the transcriptional changes in most genes, including many key regulators, were gradual. For example, the expression of the T lineage commitment factor *Bcl11b* [32, 36, 37] not only increased from DN2a to DN2b when commitment actually occurs, but also before (ETP to DN2a) and after (DN2b to DN3a) (Supplementary Fig. 1**).** The gradual nature of gene expression changes was a common feature throughout early T cell differentiation (see below) and may indicate that these transitions are not 'radical' events but rather proceed by degrees or, more prosaically, that they are not synchronized with changes in the few cell surface markers used to identify differentiation intermediates.

To group those transcripts with similar behavior during early thymocyte differentiation, we applied k-means clustering to a set of 2088 most variable genes. The resulting clusters (Fig.

2a-b, Supplementary Table 2; clusters named by a characteristic gene or group of genes) included genes with previously assigned functions in thymocyte differentiation (e.g. about half of the probes for "*Tcf-1* and *Lef-1*" and "*Cd4* and *Cd8*" clusters), but also numerous genes whose function was not previously studied in T cells, providing a rich resource for discovering novel molecular players in thymocyte differentiation.

An important feature of early T-cell differentiation is the shutdown of progenitor and non-T lineage programs [38]. The "*c-Kit*", "*Cd34*" and "PU.1" clusters (Fig. 2a-b, Supplementary Table 2) contained genes that were gradually downregulated from haematopoietic stem cells to DN3, including haematopoietic progenitor cell markers such as *Flt3, Cd34, Ly6a* (Sca-1) and *Kit,* as well as a small group of genes typical of non-T cell lineages (B, NK or myeloid). Transcriptional regulators that fell into these clusters included *Bcl11a, Hhex, Jun, Meis1, Mef2c*, and *Sfpi1* (PU.1) (Fig. 2c).

Commitment to the T cell lineage is associated with the rearrangement of *Tcrb, Tcrg* and *Tcrd* loci and induction of TCR signaling machinery. The "*Gata-3*" and "*Tcf-1* and *Lef-1*" clusters that were upregulated in early thymocytes and plateaued around the DN3a stage of T cell differentiation (Fig. 2a-b) included recombination genes (*Rag1* and *Lig4*) and a major subset of genes related to TCR signaling (*Cd3d, Cd3e, Cd3g, Lck, Itk, Grap2* (GADS), *Rasgrp1, Zap70, Cbl*, and *Nck2*) (Supplementary Fig. 2**)**. Several intriguing genes encoding proteins with likely signaling functions also fell into these clusters (Fig. 2b). For example, *Arpp21* encodes RCS, a competitive inhibitor of calmodulin-dependent enzymes, including calcineurin [39] and is thus a putative negative regulator of TCR signaling [40]. Diacylglycerol (DAG) kinase epsilon (*Dgke*) that converts DAG to phosphatidic acid may also regulate TCR signaling at this stage, as was suggested for DAG kinases alpha and zeta [41, 42]. More generally, there were interesting shifts in the entire DGK family during thymocyte differentiation (Fig. 2d).

NOTCH signaling is necessary for commitment to the T cell lineage and is indispensable at all steps of T cell differentiation prior to the DP stage [8, 9]. Direct NOTCH targets were distributed across multiple clusters with very different patterns of expression. Many canonical NOTCH targets, such as *Ptcra* (preTCRα) [43, 44], *Dtx1, Il7r* [45] and *Notch1* itself [46] fell into "preTCRα" and "*Il7r*" clusters that peak around DN3a stage (Fig 2a), consistent with the notion that DN3a cells receive the highest level of NOTCH signaling [46, 47]. A few targets, like *Nrarp* and *Hes1* (in corresponding clusters), were upregulated and plateaued as early as in ETP thymocytes (Fig 2a). Two NOTCH targets of particular interest were the transcription factors *Tcf7* [48, 49] and *Bcl11b* [32, 36, 37] (both in "*Tcf-1* and *Lef-1*" cluster). These genes were upregulated early on, plateaued by the DN3a stage, then were maintained at a high level of expression, even upon downmodulation of NOTCH signaling following β-selection. Thus, NOTCH signaling is required for induction, but not maintenance, of these key regulators of T cell differentiation, consistent with the finding that NOTCH is required early in T cell differentiation but is dispensable for maintenance of T cell identity. Finally, *Myc* [50] (from the "*c-Myc*" cluster) exhibited yet another pattern with steady expression early on and an abrupt drop in DP thymocytes. It is therefore very likely that additional factors other than NOTCH regulate expression of NOTCH targets resulting in the observed diversity of expression patterns in early thymocyte differentiation.

β-selection-induced T cell program

Expression of a productively rearranged *Tcrb* locus complexed with the germline-encoded preTCRα chain (preTCR) by DN3 thymocytes allows 'β-selection', a process that drives a burst of proliferation and phenotypic progression to the DN4 (with the downregulation of CD25), ISP (with the upregulation of CD8), and DP stages (with the upregulation of both CD4 and CD8 co-receptors) [51]. The upregulation of CD28 is one of the earliest marks of β-

selection, occurring prior to the complete downregulation of CD25, thus distinguishing post β-selected DN3b cells from non-selected DN3a cells [12]. The transition from the DN3a to DN3b stage was associated with one of the most prominent shifts in the thymocyte transcriptome (Fig. 1c-e). Much of this change was related to proliferation (>48%) (Fig. 3a) or metabolism (data not shown). Known components of the β-selection program were also included in the "*TCRα*" and "*Cd4* and *Cd8*" clusters (e.g. *Cd4, Cd8a, Cd8b1, Rorc*), along with several regulators not previously recognized in the context of thymocyte differentiation (*Chd1, Klf7, Mef2a, Meir1, Pou6f1*, and *Suhw4* (*Zfp280d*) (Fig. 2b-c).

Do all TCR-mediated signals proceed similarly? We analyzed the overlap between genes induced by signaling from the preTCR (DN3a to DN3b transition) or the αβTCR in immature DP thymocytes (small DP to CD69$^+$ DP transition) or in peripheral T cells (CD8 T cells from unchallenged versus Listeria-OVA challenged OTI mice) to determine whether a common transcriptional program was engaged downstream of these receptors at various stages of T cell differentiation. Proliferation signature genes were strongly induced by both the preTCR at the DN3 stage and the αβTCR in peripheral T cells, but not in DP thymocytes, and were therefore excluded from this analysis (Fig. 3b). Unexpectedly, transcriptional programs induced by β-selection and peripheral T cell activation were largely overlapping, with very few genes selectively induced by the preTCR, among which were *Rorc, Zap70, Cd8, Etv5* and *Ikzf3*, for example. In contrast, TCR signaling at the DP stage appeared to be very distinct from the β-selection transcriptional program. Several markers of TCR signal strength (*Cd69, Cd5, Nr4a1*) were induced downstream of both the preTCR and the αβTCR in DN and DP thymocytes, respectively, but the magnitude of their induction was lower during β-selection (Fig. 3b).

PreTCR signals are known to antagonize NOTCH signaling [46, 47]. Accordingly, a wide array of NOTCH pathway components were downregulated upon β-selection (Fig. 3a): the *Notch1* and *Notch3* receptors themselves; *Lfng,* a glycosyltransferase that enhances sensitivity of NOTCH receptors to Delta-like ligands; *Maml2,* a NOTCH transcriptional coactivator; *Dtx1, Dtx3* and *Dtx3l*, which are members of Deltex family of NOTCH regulators; and NOTCH targets, *Hes1, Il2ra, Ptcra* (preTCRα) [44]. Other NOTCH targets, like *Il7r* [45, 50] and *Myc* [14, 50, 52], were also downregulated at the transcriptional level, but with delayed kinetics (Fig. 3c). The delayed downregulation of Myc was also observed at the protein level (Fig. 3d). MYC protein amounts actually increased 3-fold following β-selection, in accordance with its mitogenic role at the β-selection checkpoint [14, 50, 52, 53], then was virtually undetectable by the DP stage. This drop in protein level was first observed at the ISP stage without a strong decrease at the mRNA level (Fig. 3d), a divergence which coincided with the upregulation of several of MYC post-transcriptional and functional regulators: *Trpc4ap,* which targets MYC for ubiquitination [54]; *Mxi1* and *Sin3b*, which antagonize transactivation functions of c-MYC/MAX dimers [55, 56] (Fig. 3d). Altogether, these observations hinted at post-transcriptional mechanisms that regulate MYC expression.

In addition to MYC activity [53], the burst of proliferation triggered by β-selection requires both preTCR and NOTCH signaling [57, 58] and is augmented by IL-7R signals. Yet, preTCR expression shut down NOTCH signaling and therefore negatively regulated these mitogenic pathways. Thus, this delayed shutdown may serve as a molecular timer that sets in motion the transcriptional changes ultimately associated with transition to the quiescent small DP stage (Fig. 3e). Accordingly, when *Myc* expression shutdown was prevented by ectopic expression of *Myc* at the DP stage, DP thymocytes failed to acquire the small cell size characteristic of the resting small DP stage **(**Supplementary Fig. 3a**)**. The positive correlation between *Myc* expression and the size of DP cells **(**Supplementary Fig. 3b**)** indicated that *Myc* downregulation may be one of the key molecular events driving the transition towards the quiescent small DP phenotype. Consistent with these results, both deletion of *Myc* and

transgenic expression of the MYC-inhibitor MAD1 at the DN3 stage led to a marked decrease in thymocyte cell size [53, 59].

Small DP cells

Transition from the DP blast to the small DP stage was associated with the most drastic change to the thymocyte transcriptome. An unusual feature of this shift was that many more genes appeared downregulated (1448 probes with FoldChange (FC) <0.5) than upregulated (225 probes with FC>2) (Fig. 1e). Much of this transcriptional shutdown affected genes involved in proliferation and various housekeeping activities such as translation, RNA processing and numerous metabolic processes (Supplementary Fig. 4 and data not shown). This observation was exemplified by the downregulation of the ribosomal protein S6 (a part of 40S ribosomal subunit) at the transcriptional and protein level (Supplementary Fig. 5).

The broad shutdown of metabolism-related genes in small DP was not merely a result of cell-cycle exit. When the expression of genes from the metabolism and proliferation-related gene ontology (GO) categories were simultaneously analyzed across the entire ImmGen dataset, many populations exhibited the expected 'low proliferation' phenotype (Fig. 4a**, bottom)**, but very few the 'low metabolism' signature (Fig. 4a**, top)**. Cell types that shutdown their metabolism-related transcriptome to a similar extent to small DP included T cells at the contraction phase of the immune response, neutrophils, microglia and red pulp macrophages (Fig. 4a-b). Neutrophils, like small DP thymocytes, have a lifespan of several days and have reduced transcription and translation activities and few mitochondria [60]. Fraction D pre-B cells also undergo a similar shutdown of metabolism and proliferation-related genes (although to a lesser extent) (Fig. 4a) and, like small DP cells, are on the cusp of an antigen receptor-controlled checkpoint. Given that huge numbers of cells within these subsets are destined to die due to the failure to express a 'useful' antigen receptor, acquisition of this 'low metabolism state' may be an adaptation that reduces the energy cost of the inevitable waste in generating an adaptive immune system.

MYC was recently described as a global amplifier of transcription driven by RNA polymerases I and III [61]. Therefore, the strong downregulation of *Myc* expression and parallel upregulation of MYC negative regulators at the small DP stage (Fig. 3d) suggested that the extent of the transcriptional shutdown may be even greater than surmised after normalization of microarray data, which only assesses relative amounts of transcripts in a cell, but can miss widespread variation [62]. To test this hypothesis, we quantified total RNA levels by cytometric analysis of pyronin Y staining **(**Fig. 4c**)**. RNA content was decreased in small DP cells compared to neighboring subsets (DN, DP blast, CD4SP and CD8SP), in accord with a previous report that detected ten times less total RNA in small DP thymocytes relative to DN4 cells [63]. We also assessed actual transcription *via* 5-Ethynyl Uridine (eU) incorporation. An abrupt decrease in *de novo* RNA synthesis occurred at the small DP stage and was thus a major contributor to the transcriptional shutdown observed in small DP cells. Altogether, these data indicated that RNA transcription was globally suppressed at the small DP stage, and that genes associated with metabolic and housekeeping activities were disproportionally affected during this shutdown.

CD69$^+$ DP, crossroad of multiple fates

Small DP cells audition for positive selection by scanning for self-peptide-MHC interactions with their newly rearranged αβTCR [64]. DP thymocytes that receive a TCR signal following pMHC engagement upregulate CD69 [65]. The small DP to CD69$^+$ DP transition was associated with the second most dramatic change in transcriptome throughout thymocyte differentiation. Accordingly, side-by-side comparison of the CD69$^+$ DP and small DP gene expression profiles revealed a large number of differentially expressed genes (Fig. 5a). As

expected, a major part of the program induced in CD69$^+$ DP thymocytes was composed of early, generic TCR activation genes, as shown by the clear partition of the signature genes characterizing TCR-stimulated DP thymocytes (Fig. 5a). Most of these TCR-related genes (75% of the upregulated signature genes) were not DP-specific as they were shared with other instances of TCR signaling, in particular in peripheral T cells (data not shown), and thus belonged to generic branches of TCR-controlled gene networks. Accordingly, a large number of immediate early response genes and canonical TCR transcriptional regulators (including NFAT, NF-κb, EGR, FOS, REL, NUR77 family members) were present among the upregulated signature genes (Fig. 5a).

Analysis of transcriptional regulators that were not part of this signature (Fig. 5b) revealed genes with possible functions in thymic positive selection. For instance, the genes encoding the inhibitory molecules ID2 and ID3, proposed to relieve the differentiation blockade enforced at the DP stage by E-proteins [66-68], were markedly upregulated in CD69$^+$ DP thymocytes. Symmetrically, *Tcf12* transcription (encoding HEB) was strongly downregulated (Fig. 5b **and** Supplementary Fig.1). Another hallmark of positive selection was the 4-fold upregulation of the recently described MHC class I transactivator, *Nlrc5* [69] (Fig. 5b). Although expression levels of MHC-I molecules were markedly impaired in *Nlrc5*-deficient mice (Fig. 5c), the increase upon positive selection was largely parallel in WT and *Nlrc5*-deficient mice, indicating that other factors modulate MHC class I expression at this step. Many of the other transcriptional regulators have no reported function in thymic differentiation and warrant future exploration (Fig. 5b).

Gene ontology and manual curation of the fraction of the CD69$^+$ DP transcriptome that was not part of the generic TCR activation signature identified several other enriched functional categories (Supplementary Fig. 6 **and** Supplementary Table 3). In particular, the "metabolic" category represented 11% of the induced genes, with genes involved in several major biosynthetic and oxidative pathways. The tricarboxylic acid cycle emerged as a critical metabolic hub in the transition from small DP to CD69$^+$ DP, with concerted transcriptional regulation of key regulators of the pyruvate dehydrogenase complex (PDH). CD69$^+$ DP thymocytes downregulated two of the most active PDK isozymes (*Pdk1* and *Pdk2*), kinases that catalyze the phosphorylation and inactivation of the PDH complex, and simultaneously increased the expression of *Pdp1* and *Pdp2* phosphatases that catalyze the opposite reaction (Fig. 5d). In addition to this coordinate regulation of *Pdk* and *Pdp* (which is also observed in starving cells [70]), CD69$^+$ DP thymocytes reactivated the upstream glycolytic pathway (Fig. 5d), with the upregulation of *Pgam1* (the most abundant 3-phosphoglycerate mutase in thymocytes) and the downregulation of *Pgm2l1* (Glu-1,6-biP synthase, whose reaction product negatively regulates hexokinase isozymes) [71].

This metabolic switch was also associated with the reactivation of other cellular housekeeping activities, which altogether composed almost 30% of the upregulated transcriptome that was not part of the early TCR activation signature. These included the restoration of active protein synthesis (representing 10% of upregulated genes); nucleocytoplasmic transport (2%); and cytoskeleton-based motility (6%) (Supplementary Fig. 6 **and** Supplementary Table 3). One revealing example was the upregulation of 20 ribosome structural proteins and key regulators of translation, such as the ribosomal S6 kinase (*Rps6ka1*) (Fig. 5e). Importantly, for most of the genes in these categories, the upregulation was only partial at the CD69$^+$ DP stage (Fig. 5e), and only completed by the mature SP stages. This step-wise reactivation was also reflected in cellular RNA content, as well as transcriptional rates, which were only gradually increased during the differentiation of DP thymocytes into mature SP cells (Fig. 4c-d). Therefore, rather than a simple shift in the balance of pro- and anti-apoptotic factors, the CD69$^+$ DP stage was characterized by the reactivation of most cellular housekeeping functions downregulated at the small DP stage.

Is there evidence of negative selection in the DP69$^+$ cell transcriptome? Although it is generally accepted that expression of CD69 identifies DP thymocytes recently engaged in positively-selecting TCR-pMHC interactions [3, 65], it is not clear which (if any) fraction of TCR-triggered CD69$^+$ DP thymocytes is doomed to die following TCR engagement with negatively-selecting pMHC ligands [72-77]. To address this question, we highlighted those genes that have been reproducibly associated with negative selection in TCR transgenic models (*Nr4a1* (NUR77), *Bcl2l11* (BIM), *Pdcd1* (PD1), and *Gadd45b* [29, 30, 78]) on a volcano plot comparing the CD69$^+$ DP and small DP stages (Fig. 6a). These genes were strongly induced in CD69$^+$ DP cells, suggesting that negative selection may indeed have a substantial footprint on the transcriptome of CD69$^+$ DP thymocytes.

To determine whether we could distinguish positive and negative selection at the transcriptional level, we next compared the transcriptomes of CD69$^+$ DP and CD4$^+$CD8^{int} (intermediate CD4SP) thymocytes, which correspond to the earliest positively selected cell population that ultimately gives rise to both CD4 and CD8 lineages [7] (Fig. 6b). As expected, the vast majority of genes upregulated in CD69$^+$ DP thymocytes showed similar expression in CD4$^+$CD8^{int} cells (e.g., *Cd53, Bcl2* and *H2-k1*), confirming that positive selection was a major contributor to the CD69$^+$ DP transcriptome. However, a subset of the upregulated genes was more highly expressed in CD69$^+$ DP than in intermediate CD4SP (*e.g., Nr4a1, Gadd45b, Pdcd1*, and *Bcl2l11*), or vice-versa (*e.g., Nlrc5, Il7r*, and *Gimap3/4*). This divergence of the transcriptional profiles suggested putative markers associated with positive and negative selection.

We thus explored the expression of some of these markers by flow cytometry to determine whether a subset of CD69$^+$ DP cells was associated with apoptosis. The combined use of antibodies directed against MHC class I (upregulation of which was one transcriptional hallmark of positively selected cells observed in Fig. 6b, e.g. *H2-k1*) and CD69 subdivided thymocytes into 5 clear subpopulations (see Supplementary Fig. 7 for gating strategy). Two distinct phenotypes could be discerned in the CD69^{hi}MHCI^{neg} thymocyte fraction (Fig. 6c). The CD4^{dull}CD8^{dull} subset contained a high proportion of cells with high levels of NR4A1, PD-1, and HELIOS (encoded by *Ikzf2*) and little or no BCL2 and IL-7R (Fig. 6d). In contrast, the CD4$^+$CD8^{int} subset showed exactly opposite expression patterns for these markers (Fig. 6d). These results suggested that the CD4^{dull}CD8^{dull}CD69^{hi}MHCI^{neg} subset was enriched in cells at an early stage of deletion by apoptosis.

To test this hypothesis, we analyzed the activation of Caspase-3 (Fig. 6e). Interestingly, the CD4^{dull}CD8^{dull} population had a singularly high frequency of activated Caspase-3$^+$ cells (up to 3%), even when compared with immature SP populations, known to be sensitive to clonal deletion (Fig. 6e and Supplementary Fig. 7). Note that activated Caspase-3$^+$ cells in the CD4^{dull}CD8^{dull} population included CD69^{neg} and CD69^{hi} cells, which were both markedly decreased in MHC class I and II-deficient mice (by 10 and 100-fold) and in *Bim*-deficient mice (by 4-fold) (Fig. 6e-f), thereby identifying a DP thymocyte subset in unmanipulated mice undergoing cell death in a MHC- and Bim-dependent manner, which is characteristic of *bona-fide* clonal deletion. Small DP cells also contained a significant proportion of CD69^{neg} activated Caspase-3$^+$ cells, which, in contrast to the CD4^{dull}CD8^{dull} population, was increased in the absence of MHC class I and II molecules (Fig. 6f), likely identifying cells dying by neglect. Altogether, these observations revealed a surprisingly large deletional program within the polyclonal repertoire of DP thymocytes.

Differentiation of CD4 and CD8 lineages

The above results indicated that the CD69$^+$ DP subset was a heterogeneous population, with only a fraction of the cells differentiating from the DP to SP stage. This differentiation event comprised one of the largest changes observed during thymocyte differentiation, with

variations in the expression of more than 2600 gene probes (Fig. 1e and Fig. 7a). Despite the scale of this transcriptome shift, most of the changes were common for both CD4 and CD8 lineages (approximately 93%), with surprisingly few genes differentially expressed (Fig. 7a). Among these, *Cd40l* and *Tnfrsf4* (OX40) were specifically upregulated in the CD4 lineage, while *Crtam* and *Cd226* genes, associated with granule- and IFN-γ-mediated cytotoxic functions [79], were more highly expressed in the CD8 lineage. Correspondingly, very few transcriptional regulators were differentially expressed, exemplified by the well-described *Zbtb7b* (THPOK) and *Gata3* on the CD4 side, *Runx3* and *Eomes* on the CD8 side [80] (Fig. 7b). Thus, the CD4 and CD8 lineages are distinguished by surprisingly few transcriptional marks during thymocyte differentiation.

Thymic egress is coupled with a phase of functional maturation [23]. To test the hypothesis that this maturation phase could reinforce lineage identities and further demarcate their transcriptomes, we compared thymic and peripheral T cells (Fig. 8a). Surprisingly, little evidence of such a maturation process was observed at the transcriptional level. Most downregulated genes were cell-cycle-related and probably reflected the small fraction of proliferating mature SP thymocytes [81]. Only 12 genes showed a significant upregulation in peripheral T cells relative to mature thymic counterparts (with a FC threshold of 2) (Fig. 8a). One of these genes was *Cd55*, whose gene product deactivates complement C3 convertases and protects cells from the lytic action of complement, while the function of another, *Dapl1*, is unknown in T cells. The upregulation of these genes upon thymic egress was similar in CD4 and CD8 lineages (Fig. 8a). Finally, a small subset of genes selectively downregulated in peripheral $CD4^+$ T cells reflected the inclusion of Treg cells in the thymic, but not the lymph node, $CD4^+$ subset. These observations demonstrated that thymic egress had limited transcriptional consequences, with no reinforcement of CD4 and CD8 lineage identities.

What ultimately defines lineage identities in peripheral T cells? In line with the thymocyte profiling, a direct comparison of peripheral $CD4^+$ and $CD8^+$ T cells revealed few differentially expressed gene probes (159 at a FC threshold of 2, FDR<10^{-4}), most of which overlapped with those previously detected in thymocytes (Fig. 8b). A few of these genes were associated with TCR signaling functions: *Cd28, Trib2* (a negative regulator of MAPK), and *Mapk11* (p38beta) on the $CD4^+$ side; *Dpp4* (CD26) and *Rnf125* (a positive regulator of T cell activation) on the $CD8^+$ side. Such limited divergence is surprising, given the physiologically distinct functions of $CD4^+$ and $CD8^+$ T cells. We reasoned that these modest differences in the baseline transcriptomes might be amplified upon activation and/or reflected in post-translational cascades during activation.

Therefore, we compared TCR signaling events in $CD4^+$ and $CD8^+$ T cells using multidimensional mass cytometry (CyTOF) [34]. Lymph node cell suspensions were stimulated with anti-CD3 and -CD28 antibodies and interrogated for the phosphorylation status of 15 intracellular signaling molecules and the expression of 7 cell surface markers, across 15 time-points (Fig. 8c). Despite a slightly higher level of phosphorylation in $CD4^+$ T cells, most key TCR-proximal (CD3ζ, ZAP-70, LAT, SLP-76) and downstream nodes (ERK1/2, S6, MAPKAPKII, NF-κB) had very similar dynamics of phosphorylation in $CD4^+$ and $CD8^+$ T cells, mirroring the transcriptional similarity. We also isolated anti-CD3 and anti-CD28-stimulated $CD4^+$ and $CD8^+$ peripheral T cells for gene expression profiling (Fig. 8d). Reminiscent of maturation-induced changes in thymocytes, the vast majority of activation-induced changes in the transcriptomes of $CD4^+$ and $CD8^+$ cells were shared (Fig. 8d). Nonetheless, some divergence of $CD4^+$ and $CD8^+$ transcriptional programs was evident as early as one hour following TCR stimulation and, surprisingly, included lineage-specific downregulation of the master transcriptional regulators of each lineage (*Zbtb7b, Gata3, Runx3* and *Eomes*).

Transcriptional divergence of $CD4^+$ and $CD8^+$ T cells increased over time (Fig. 8d). One example was *Xcl1*, whose product attracts dendritic cells and is crucial for an efficient cytotoxic response [82]. Other chemokine genes like *Ccl3* (MIP1α) and *Ccl4* (MIP1β), as well as genes directly involved in $CD8^+$ cell functions (*Crtam* and *Gzmb*), were also selectively regulated (Fig. 8d). On the $CD4^+$ cell side, preferentially expressed genes included *Il2, Il2rb, Tnfsf4* (OX40L), *Tnfrsf4* (OX40), among others. Therefore, the great similarity between the transcriptomes of CD4 and CD8 lineages, acquired upon positive selection, persisted through peripheral migration and was reflected in their signaling and transcriptional responses to TCR stimulation. This close transcriptional similarity contrasts with our perception of their very different functions.

Discussion

Our analysis of the entire transcriptional spectrum of thymocyte differentiation states revealed several new insights. Dual control of *Myc* expression at the transcriptional and post-transcriptional levels (via the downregulation of *Mxi1, Sin3b* and *Trpc4ap*) was apparent at the small DP to $CD69^+$ DP transition, as at the β-selection checkpoint, compatible with the notion that MYC constitutes the cellular rheostat that enforces the programmed starving at the small DP stage and the reactivation of cellular functions upon positive selection. Although the precise function of MYC at this stage remains to be investigated, several lines of evidence argue in favor of this possibility. First, the inhibition of MYC activity *via* the overexpression of MYC-inhibitor MAD1 led to a decreased cell size of SP thymocytes, as well as a decrease in the proportion of $CD3^{hi}$ mature SP thymocytes [59]. Second, although no phenotype was reported in mice overexpressing or deleting *Myc* at the DP stage in polyclonal settings [53, 83], *Myc* overexpression in DP thymocytes of HY TCR transgenic mice led to a significant increase in positive selection efficiency [83].

The expression of a complete αβTCR renders DP thymocytes eligible for positive selection. Whether significant levels of negative selection also occur at this stage in an unmanipulated, polyclonal setting has been a controversial question. Our expression profiling uncovered a program associated with apoptotic deletion within the early $CD69^+$ DP subset, a consequence of their first TCR-pMHC interactions. By tracking a variety of proteins identified through this transition, we could ascribe this program to a subset of $CD69^{hi}MHCI^{neg}$ DP thymocytes with activated CCaspase-3, identifying a distinct fraction of DP undergoing deletion. Future studies that take into account the dynamics of this process will be required to more precisely quantify this early wave of cortical deletion relative to negative selection in the thymic medulla.

This Resource also provides an important reference for T-cell diseases such leukemia, immunodeficiency and autoimmunity. The transcriptomes of each thymocyte subset allows for more precise staging of malignancies or identifying how differentiation stalls in the context of transcriptional networks. For example, a recent study found that T-cell acute lymphoblastic leukemia induced by *Tcf-1*-deficiency was, in fact, driven by dysregulation of *Lef-1* [84], highlighting the interdependence of the transcription factors driving early thymocyte differentiation. Furthermore, the definition of the normal dynamic of transcriptional regulation throughout thymocyte differentiation will enable the identification of the origins of network perturbations in disease-relevant models.

In conclusion, the comprehensive resolution of αβ T cell transcriptomes through the entire course of their differentiation yields a unique perspective that colors somewhat differently our appreciation of differentiative events: the apparently gradual nature of commitment to the T cell lineage, the deep shutdown of cortical DP thymocytes followed by cellular

reactivation upon positive selection, the quasi-identity of $CD4^+$ and $CD8^+$ T cells. We were able to take stock of the uncharted space across key transitions in thymocyte differentiation and highlight many interesting candidate genes that are unexplored in T cells. Very few of the transcriptional regulators identified through the DP transitions have been analyzed, while almost all of the [rare] transcription factors differentially expressed between $CD4^+$ and $CD8^+$ T cells have already been characterized. Thus, this analysis sets the boundaries of the "known unknown" in αβT cell differentiation and the challenge now is to integrate these with the "knowns" for a more complete view of T cell biology.

Supplementary Material

Refer to Web version on PubMed Central for supplementary material.

Acknowledgments

We thank Ananda Goldrath and Joonsoo Kang for critical reading of the manuscript, K. Hattori, A. Ortiz-Lopez, and N. Asinovski for mice and antibodies, J. Moore, and A. Kressler for flow cytometry, and C. Laplace for assistance with figure preparation. This work was supported by grant AI072073 from the NIH. MM was supported by a postdoctoral fellowship from the Human Frontier Science Program (HFSP-LT000096), DG by a NH&MRC Career Development Fellowship (637353), TH by an ARC Australian Postdoctoral Research Fellowship (Industry) (LP110201169).

References

1. Miller JF. The golden anniversary of the thymus. Nat Rev. Immunol. 2011; 11:489–495. [PubMed: 21617694]
2. von Boehmer H, Teh HS, Kisielow P. The thymus selects the useful, neglects the useless and destroys the harmful. Immunol. Today. 1989; 10:57–61. [PubMed: 2526642]
3. Jameson SC, Hogquist KA, Bevan MJ. Positive selection of thymocytes. Annu. Rev. Immunol. 1995; 13:93–126. [PubMed: 7612239]
4. Robey E. Regulation of T cell fate by Notch. Annu. Rev. Immunol. 1999; 17:283–295. [PubMed: 10358760]
5. Hogquist KA, Baldwin TA, Jameson SC. Central tolerance: learning self-control in the thymus. Nat. Rev. Immunol. 2005; 5:772–782. [PubMed: 16200080]
6. Stritesky GL, Jameson SC, Hogquist KA. Selection of self-reactive T cells in the thymus. Annu. Rev. Immunol. 2012; 30:95–114. [PubMed: 22149933]
7. Singer A, Adoro S, Park JH. Lineage fate and intense debate: myths, models and mechanisms of CD4- versus CD8-lineage choice. Nat Rev. Immunol. 2008; 8:788–801. [PubMed: 18802443]
8. Thompson PK, Zuniga-Pflucker JC. On becoming a T cell, a convergence of factors kick it up a Notch along the way. Semin. Immunol. 2011; 23:350–359. [PubMed: 21981947]
9. Rothenberg EV. T cell lineage commitment: identity and renunciation. J Immunol. 2011; 186:6649–6655. [PubMed: 21646301]
10. Godfrey DI, Kennedy J, Suda T, Zlotnik A. A developmental pathway involving four phenotypically and functionally distinct subsets of $CD3^-CD4^-CD8^-$ triple-negative adult mouse thymocytes defined by CD44 and CD25 expression. J. Immunol. 1993; 150:4244–4252. [PubMed: 8387091]
11. Bhandoola A, von BH, Petrie HT, Zuniga-Pflucker JC. Commitment and developmental potential of extrathymic and intrathymic T cell precursors: plenty to choose from. Immunity. 2007; 26:678–689. [PubMed: 17582341]
12. Williams JA, et al. Regulated costimulation in the thymus is critical for T cell development: dysregulated CD28 costimulation can bypass the pre-TCR checkpoint. J Immunol. 2005; 175:4199–4207. [PubMed: 16177059]
13. Prinz I, et al. Visualization of the earliest steps of gammadelta T cell development in the adult thymus. Nat Immunol. 2006; 7:995–1003. [PubMed: 16878135]

14. Kreslavsky T, et al. beta-Selection-Induced Proliferation Is Required for alphabeta T Cell Differentiation. Immunity. 2012; 37:840–853. [PubMed: 23159226]
15. Zinkernagel RM, Callahan GN, Klein J, Dennert G. Cytotoxic T cells learn specificity for self H-2 during diffentiation in the thymus. Nature. 1978; 271:251–253. [PubMed: 304527]
16. MacDonald HR, et al. Positive selection of CD4+ thymocytes controlled by MHC class II gene products. Nature. 1988; 336:471–473. [PubMed: 3264054]
17. Kisielow P, Teh HS, Bluthmann H, von Boehmer H. Positive selection of antigen-specific T cells in thymus by restricting MHC molecules. Nature. 1988; 335:730–733. [PubMed: 3262831]
18. Bousso P, Bhakta NR, Lewis RS, Robey E. Dynamics of thymocyte-stromal cell interactions visualized by two-photon microscopy. Science. 2002; 296:1876–1880. [PubMed: 12052962]
19. Egerton M, Scollay R, Shortman K. Kinetics of mature T-cell development in the thymus. Proc. Natl. Acad. Sci. U. S. A. 1990; 87:2579–2582. [PubMed: 2138780]
20. Teh HS, et al. Thymic major histocompatibility complex antigens and the alpha beta T-cell receptor determine the CD4/CD8 phenotype of T cells. Nature. 1988; 335:229–233. [PubMed: 2970593]
21. Jordan MS, et al. Thymic selection of CD4+CD25+ regulatory T cells induced by an agonist self-peptide. Nat. Immunol. 2001; 2:283–284. [PubMed: 11276194]
22. Leishman AJ, et al. Precursors of functional MHC class I- or class II-restricted CD8alphaalpha(+) T cells are positively selected in the thymus by agonist self-peptides. Immunity. 2002; 16:355–364. [PubMed: 11911821]
23. Fink PJ, Hendricks DW. Post-thymic maturation: young T cells assert their individuality. Nat Rev. Immunol. 2011; 11:544–549. [PubMed: 21779032]
24. DeRyckere D, Mann DL, DeGregori J. Characterization of transcriptional regulation during negative selection in vivo. J Immunol. 2003; 171:802–811. [PubMed: 12847248]
25. Schmitz I, Clayton LK, Reinherz EL. Gene expression analysis of thymocyte selection in vivo. Int. Immunol. 2003; 15:1237–1248. [PubMed: 13679393]
26. Liston A, et al. Generalized resistance to thymic deletion in the NOD mouse; a polygenic trait characterized by defective induction of Bim. Immunity. 2004; 21:817–830. [PubMed: 15589170]
27. Mick VE, et al. The regulated expression of a diverse set of genes during thymocyte positive selection in vivo. J Immunol. 2004; 173:5434–5444. [PubMed: 15494490]
28. Zucchelli S, et al. Defective central tolerance induction in NOD mice: genomics and genetics. Immunity. 2005; 22:385–396. [PubMed: 15780994]
29. Baldwin TA, Hogquist KA. Transcriptional analysis of clonal deletion in vivo. J. Immunol. 2007; 179:837–844. [PubMed: 17617574]
30. Mingueneau M, et al. Thymic negative selection is functional in NOD mice. J Exp. Med. 2012
31. Zhang JA, et al. Dynamic transformations of genome-wide epigenetic marking and transcriptional control establish T cell identity. Cell. 2012; 149:467–482. [PubMed: 22500808]
32. Li L, Leid M, Rothenberg EV. An early T cell lineage commitment checkpoint dependent on the transcription factor Bcl11b. Science. 2010; 329:89–93. [PubMed: 20595614]
33. Luc S, et al. The earliest thymic T cell progenitors sustain B cell and myeloid lineage potential. Nat Immunol. 2012; 13:412–419. [PubMed: 22344248]
34. Bendall SC, et al. Single-cell mass cytometry of differential immune and drug responses across a human hematopoietic continuum. Science. 2011; 332:687–696. [PubMed: 21551058]
35. Narayan K, et al. Intrathymic programming of effector fates in three molecularly distinct gammadelta T cell subtypes. Nat Immunol. 2012; 13:511–518. [PubMed: 22473038]
36. Ikawa T, et al. An essential developmental checkpoint for production of the T cell lineage. Science. 2010; 329:93–96. [PubMed: 20595615]
37. Li P, et al. Reprogramming of T cells to natural killer-like cells upon Bcl11b deletion. Science. 2010; 329:85–89. [PubMed: 20538915]
38. Rothenberg EV, Zhang J, Li L. Multilayered specification of the T-cell lineage fate. Immunol. Rev. 2010; 238:150–168. [PubMed: 20969591]
39. Rakhilin SV, et al. A network of control mediated by regulator of calcium/calmodulin-dependent signaling. Science. 2004; 306:698–701. [PubMed: 15499021]

40. Kisielow J, Nairn AC, Karjalainen K. TARPP, a novel protein that accompanies TCR gene rearrangement and thymocyte education. Eur. J Immunol. 2001; 31:1141–1149. [PubMed: 11298339]
41. Olenchock BA, et al. Disruption of diacylglycerol metabolism impairs the induction of T cell anergy. Nat Immunol. 2006; 7:1174–1181. [PubMed: 17028587]
42. Guo R, et al. Synergistic control of T cell development and tumor suppression by diacylglycerol kinase alpha and zeta. Proc Natl Acad Sci U S A. 2008; 105:11909–11914. [PubMed: 18689679]
43. Deftos ML, et al. Notch1 signaling promotes the maturation of CD4 and CD8 SP thymocytes. Immunity. 2000; 13:73–84. [PubMed: 10933396]
44. Reizis B, Leder P. Direct induction of T lymphocyte-specific gene expression by the mammalian Notch signaling pathway. Genes Dev. 2002; 16:295–300. [PubMed: 11825871]
45. Gonzalez-Garcia S, et al. CSL-MAML-dependent Notch1 signaling controls T lineage-specific IL-7 R{alpha} gene expression in early human thymopoiesis and leukemia. J Exp. Med. 2009; 206:779–791. [PubMed: 19349467]
46. Yashiro-Ohtani Y, et al. Pre-TCR signaling inactivates Notch1 transcription by antagonizing E2A. Genes Dev. 2009; 23:1665–1676. [PubMed: 19605688]
47. Taghon T, et al. Developmental and molecular characterization of emerging beta- and gammadelta-selected pre-T cells in the adult mouse thymus. Immunity. 2006; 24:53–64. [PubMed: 16413923]
48. Germar K, et al. T-cell factor 1 is a gatekeeper for T-cell specification in response to Notch signaling. Proc Natl Acad Sci U S A. 2011; 108:20060–20065. [PubMed: 22109558]
49. Weber BN, et al. A critical role for TCF-1 in T-lineage specification and differentiation. Nature. 2011; 476:63–68. [PubMed: 21814277]
50. Weng AP, et al. c-Myc is an important direct target of Notch1 in T-cell acute lymphoblastic leukemia/lymphoma. Genes Dev. 2006; 20:2096–2109. [PubMed: 16847353]
51. von Boehmer H. Selection of the T-cell repertoire: receptor-controlled checkpoints in T-cell development. Adv. Immunol. 2004; 84:201–238. [PubMed: 15246254]
52. Wong GW, et al. HES1 opposes a PTEN-dependent check on survival, differentiation, and proliferation of TCRbeta-selected mouse thymocytes. Blood. 2012; 120:1439–1448. [PubMed: 22649105]
53. Dose M, et al. c-Myc mediates pre-TCR-induced proliferation but not developmental progression. Blood. 2006; 108:2669–2677. [PubMed: 16788099]
54. Choi SH, Wright JB, Gerber SA, Cole MD. Myc protein is stabilized by suppression of a novel E3 ligase complex in cancer cells. Genes Dev. 2010; 24:1236–1241. [PubMed: 20551172]
55. Adhikary S, Eilers M. Transcriptional regulation and transformation by Myc proteins. Nat Rev. Mol. Cell Biol. 2005; 6:635–645. [PubMed: 16064138]
56. Schreiber-Agus N, DePinho RA. Repression by the Mad(Mxi1)-Sin3 complex. Bioessays. 1998; 20:808–818. [PubMed: 9819568]
57. Ciofani M, et al. Obligatory role for cooperative signaling by pre-TCR and Notch during thymocyte differentiation. J Immunol. 2004; 172:5230–5239. [PubMed: 15100261]
58. Maillard I, et al. The requirement for Notch signaling at the beta-selection checkpoint in vivo is absolute and independent of the pre-T cell receptor. J Exp. Med. 2006; 203:2239–2245. [PubMed: 16966428]
59. Iritani BM, et al. Modulation of T-lymphocyte development, growth and cell size by the Myc antagonist and transcriptional repressor Mad1. EMBO J. 2002; 21:4820–4830. [PubMed: 12234922]
60. Geering B, Simon HU. Peculiarities of cell death mechanisms in neutrophils. Cell Death. Differ. 2011; 18:1457–1469. [PubMed: 21637292]
61. Nie Z, et al. c-Myc is a universal amplifier of expressed genes in lymphocytes and embryonic stem cells. Cell. 2012; 151:68–79. [PubMed: 23021216]
62. Loven J, et al. Revisiting global gene expression analysis. Cell. 2012; 151:476–482. [PubMed: 23101621]
63. Neilson JR, Zheng GX, Burge CB, Sharp PA. Dynamic regulation of miRNA expression in ordered stages of cellular development. Genes. Dev. 2007; 21:578–589. [PubMed: 17344418]

64. Starr TK, Jameson SC, Hogquist KA. Positive and negative selection of T cells. Ann. Rev. Immunol. 2003; 21:139–176. [PubMed: 12414722]
65. Swat W, Dessing M, von BH, Kisielow P. CD69 expression during selection and maturation of CD4+8+ thymocytes. Eur. J Immunol. 1993; 23:739–746. [PubMed: 8095460]
66. Jones ME, Zhuang Y. Acquisition of a functional T cell receptor during T lymphocyte development is enforced by HEB and E2A transcription factors. Immunity. 2007; 27:860–870. [PubMed: 18093538]
67. Rivera RR, et al. Thymocyte selection is regulated by the helix-loop-helix inhibitor protein, Id3. Immunity. 2000; 12:17–26. [PubMed: 10661402]
68. Bain G, et al. Regulation of the helix-loop-helix proteins, E2A and Id3, by the Ras-ERK MAPK cascade. Nat Immunol. 2001; 2:165–171. [PubMed: 11175815]
69. Meissner TB, et al. NLR family member NLRC5 is a transcriptional regulator of MHC class I genes. Proc Natl Acad Sci U S A. 2010; 107:13794–13799. [PubMed: 20639463]
70. Huang B, Wu P, Popov KM, Harris RA. Starvation and diabetes reduce the amount of pyruvate dehydrogenase phosphatase in rat heart and kidney. Diabetes. 2003; 52:1371–1376. [PubMed: 12765946]
71. Maliekal P, et al. Molecular identification of mammalian phosphopentomutase and glucose-1,6-bisphosphate synthase, two members of the alpha-D-phosphohexomutase family. J Biol. Chem. 2007; 282:31844–31851. [PubMed: 17804405]
72. van Meerwijk JP, et al. Quantitative impact of thymic clonal deletion on the T cell repertoire. J Exp. Med. 1997; 185:377–383. [PubMed: 9053438]
73. Surh CD, Sprent J. T-cell apoptosis detected in situ during positive and negative selection in the thymus. Nature. 1994; 372:100–103. [PubMed: 7969401]
74. Viret C, et al. A role for accessibility to self-peptide-self-MHC complexes in intrathymic negative selection. J Immunol. 2001; 166:4429–4437. [PubMed: 11254698]
75. McCaughtry TM, Baldwin TA, Wilken MS, Hogquist KA. Clonal deletion of thymocytes can occur in the cortex with no involvement of the medulla. J Exp. Med. 2008; 205:2575–2584. [PubMed: 18936237]
76. Baldwin KK, Trenchak BP, Altman JD, Davis MM. Negative selection of T cells occurs throughout thymic development. J Immunol. 1999; 163:689–698. [PubMed: 10395659]
77. Krueger A, von Boehmer H. Identification of a T lineage-committed progenitor in adult blood. Immunity. 2007; 26:105–116. [PubMed: 17222572]
78. Liston A, et al. Impairment of organ-specific T cell negative selection by diabetes susceptibility genes: genomic analysis by mRNA profiling. Genome Biol. 2007; 8:R12. [PubMed: 17239257]
79. Chan CJ, Andrews DM, Smyth MJ. Receptors that interact with nectin and nectin-like proteins in the immunosurveillance and immunotherapy of cancer. Curr. Opin. Immunol. 2012; 24:246–251. [PubMed: 22285893]
80. Wang L, Bosselut R. CD4-CD8 lineage differentiation: Thpok-ing into the nucleus. J Immunol. 2009; 183:2903–2910. [PubMed: 19696430]
81. Penit C, Vasseur F. Expansion of mature thymocyte subsets before emigration to the periphery. J Immunol. 1997; 159:4848–4856. [PubMed: 9366410]
82. Lei Y, Takahama Y. XCL1 and XCR1 in the immune system. Microbes. Infect. 2012; 14:262–267. [PubMed: 22100876]
83. Rudolph B, Hueber AO, Evan GI. Reversible activation of c-Myc in thymocytes enhances positive selection and induces proliferation and apoptosis in vitro. Oncogene. 2000; 19:1891–1900. [PubMed: 10773879]
84. Yu S, et al. The TCF-1 and LEF-1 transcription factors have cooperative and opposing roles in T cell development and malignancy. Immunity. 2012; 37:813–826. [PubMed: 23103132]
85. Tullai JW, et al. Immediate-early and delayed primary response genes are distinct in function and genomic architecture. J Biol. Chem. 2007; 282:23981–23995. [PubMed: 17575275]

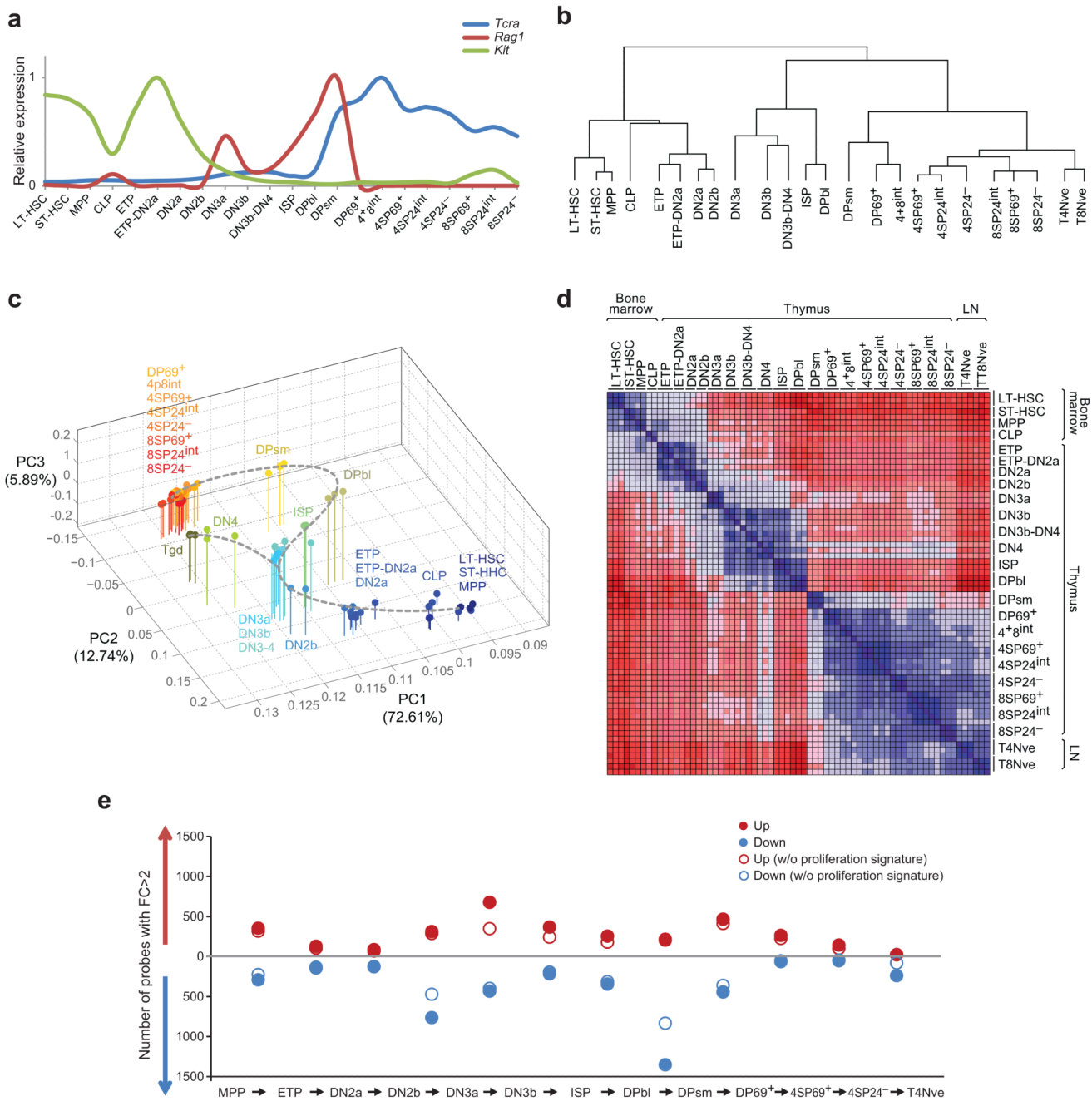

Figure 1.

Bird's-eye view of transcriptome changes in the course of T cell differentiation. **(a)** Maximum-normalized mean expression values for *Rag1, Tcra* and *Kit* in indicated BM and thymocyte populations. **(b)** Hierarchical clustering, **(c)** Principal Component Analysis and **(d)** heatmap of Euclidian distances between indicated populations, calculated using the 15% of probes with the greatest difference in expression among these subsets and with expression values over 120 for at least one of the subsets. Expression values were $\log^2$-transformed and row-standardized prior to the analysis. **(e)** Number of probes upregulated (red symbols) or downregulated (blue symbols) by 2-fold or more at the indicated transitions during T cell

differentiation. Filled symbols, total number of probes; open symbols, number of probes which are not part of the proliferation signature.

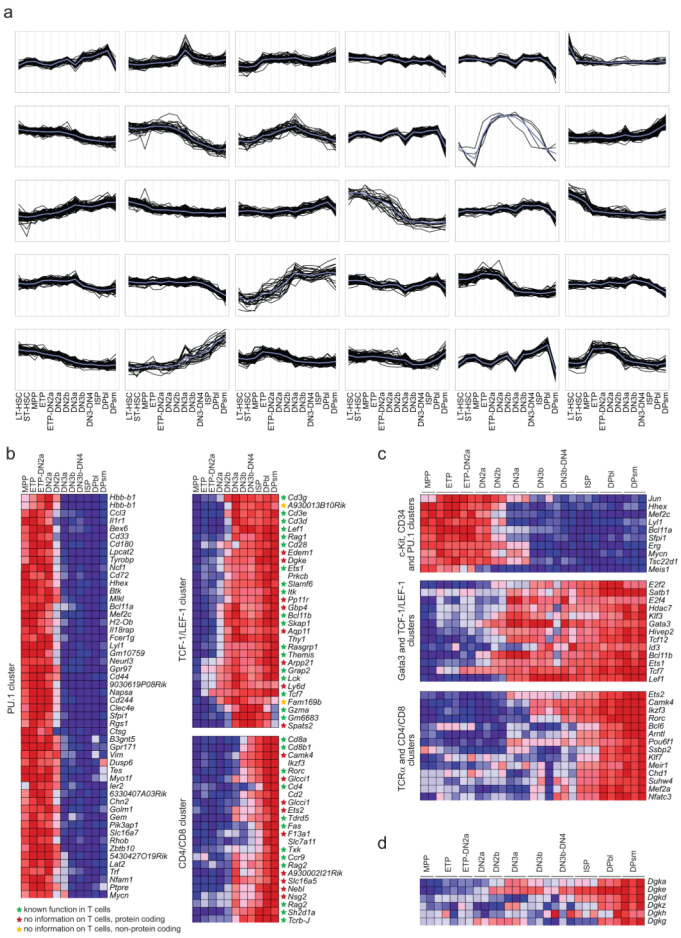

Figure 2.

Dynamics of gene expression during early T cell differentiation. K-means clusters of genes showing differential expression during early T cell differentiation. **(a)** Log^2-transformed mean-centered expression values for the genes (black lines) and cluster centroids (grey line) for each cluster. Clusters are named by a characteristic gene or group of genes in the cluster. The complete list of genes in each cluster is provided in Supplementary Table 2. **(b)** Heatmaps showing expression levels of genes from PU.1 (left), TCF-1/LEF-1 (top right), and CD4/CD8 (bottom right) clusters. **(c)** Heatmaps showing expression levels of transcriptional regulators from indicated clusters. **(d)** Heatmap showing expression levels of diacylglycerol kinase genes whose expression changed by 3-fold or more during early T cell differentiation.

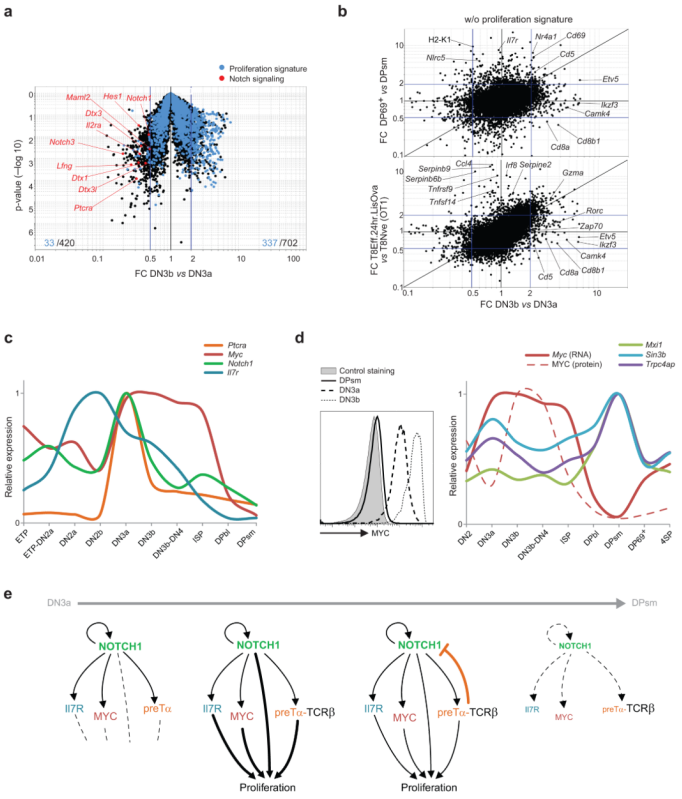

Figure 3.

Transcriptional footprint of β-selection. **(a)** Volcano plot comparing DN3b and DN3a thymocyte stages (Fold Change: x axis; t test p-value: y axis). Probes corresponding to the proliferation signature (see Methods section for definition) and components of NOTCH signaling pathway are highlighted in blue and red, respectively. **(b)** Fold change/FC plots comparing transcriptome changes induced by preTCR signaling in DN thymocytes (DN3b vs DN3a, x-axis) versus αβTCR signaling in DP thymocytes (top, $CD69^+$ DP ($DP69^+$) versus small DP (DPsm), y-axis) and in peripheral T cells (bottom, OT1 TCR transgenic cells, 24 hours after Listeria-OVA infection vs naïve OT1 cells). Blue lines mark a FC of 2. **(c)** Maximum-normalized mean expression of *Notch1* and indicated NOTCH target genes in thymocyte subsets. **(d)** Histogram showing expression levels of MYC, detected by flow cytometry (left) and maximum-normalized mRNA levels of *Myc* and negative regulators of MYC in the indicated thymocyte populations (right). MYC protein levels are indicated with a dashed line for comparison. Flow cytometry analysis of MYC expression is representative of 3 independent experiments. **(e)** Schematic of the proposed model describing the interplay between the preTCR, NOTCH1, IL-7R and MYC in T cell physiology during early T cell differentiation.

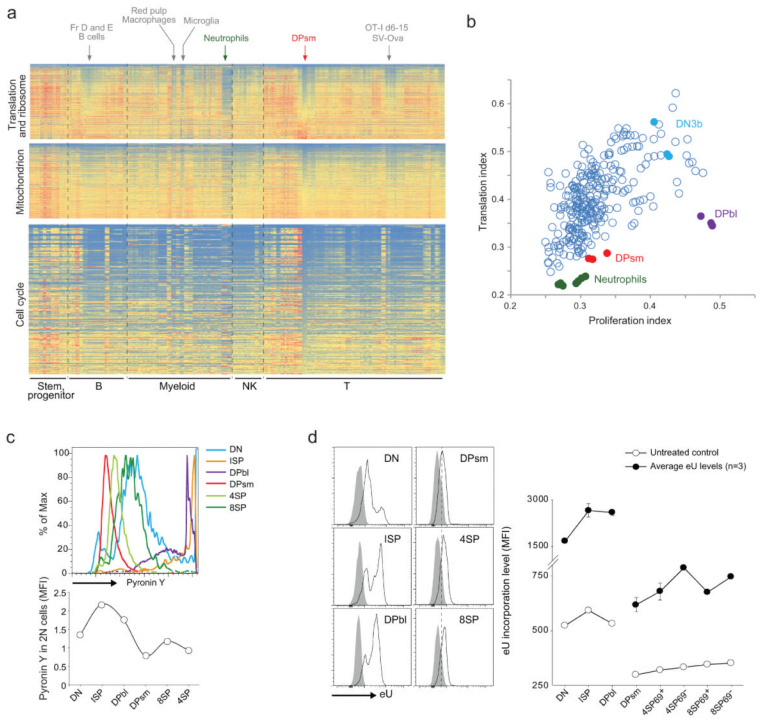

Figure 4.

Transcriptional shutdown in small DP thymocytes. **(a)** Heatmaps showing normalized expression values for probes belonging to the GO categories for: ribosome and translation (GO:0005840 and 0006412) (top); mitochondrion (GO:0005739) (middle); and cell cycle (GO:0007049) (bottom) across BM progenitor, B cell, myeloid and T cell subsets. Probes are sorted by increasing value in small DP (DPsm). **(b)** Scatter plot showing 'proliferation' and 'translation' indexes calculated by averaging row maximum-normalized expression values for each probe in the proliferation signature ('proliferation' index) or translation and ribosome categories ('translation' index), for the same set of cell populations shown in (a). **(c)** Pyronin Y quantification of total RNA content in thymocytes. Histogram overlay (top) and mean fluorescence intensity (bottom) in indicated thymocyte subsets. **(d)** Analysis of transcriptional activity via eU incorporation. Total thymocytes were incubated for 2 hrs in presence of eU nucleotide, followed by flow cytometric detection of incorporated eU by click chemistry. Representative eU saining histograms (left) and corresponding mean fluorescence intensity (right) in indicated thymocyte subsets. Panels (c) and (d) are representative of two independent experiments.

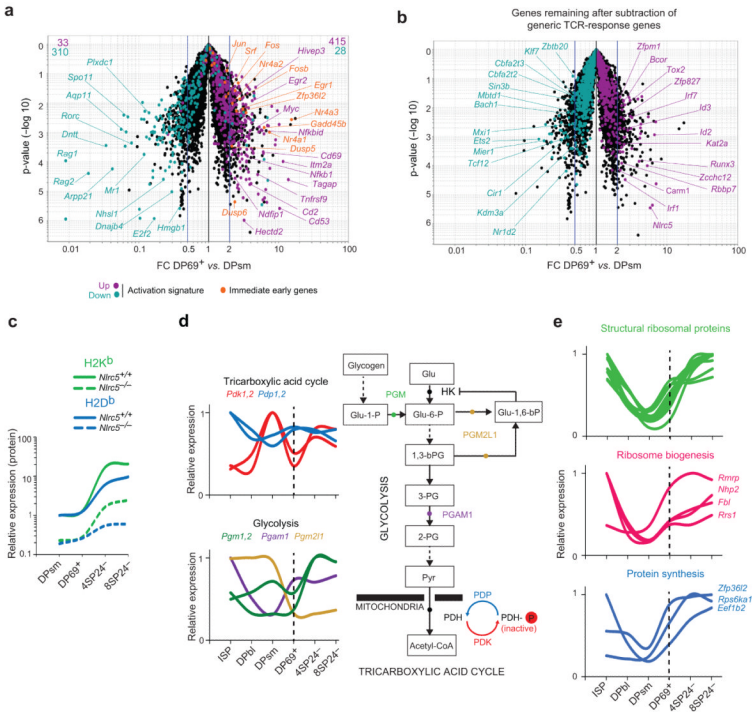

Figure 5.

Reactivation of housekeeping activities upon positive selection. **(a)** Volcano plot comparing CD69$^+$ DP (DP69$^+$) and small DP (DPsm) thymocytes (Fold Change: x axis; t test p-value: y axis). Signature genes upregulated (violet) and downregulated (cyan) at early time points following *in vitro* TCR stimulation of DP thymocytes are highlighted. Signature genes were derived from the previously described transcriptome analysis of BDC2.5 TCR transgenic DP thymocytes [30], and include all genes induced or repressed (FC threshold of 2) at 3 h or 7 h post-stimulation with mimotope-pulsed splenic APCs. The number of signature genes in the upregulated and downregulated transcriptome, are indicated. Immediate early response genes (orange) were derived from the transcriptome analysis of a PDGF-stimulated cell line [85]. **(b)** Gene probes remaining after subtraction of TCR-stimulated DP signature genes (highlighted in (a)). Transcriptional regulators upregulated (violet) and downregulated (cyan) are highlighted (using a list of 1,680 known or putative transcriptional regulators, provided in Supplementary Table 4). **(c)** Relative expression of MHC class I on indicated thymocyte subsets, detected by flow cytometry with anti-H2-K^b (green) and H2-D^b (blue) antibodies in *Nlrc5*-sufficient (solid lines), and *Nlrc5*-deficient mice (dashed lines). **(d)** Maximum-normalized mean expression of 8 metabolism-related transcripts regulated at the small DP to CD69$^+$ DP transition, whose gene-products control key steps of the glycolytic and tricarboxylic acid cycle pathways. The schematic diagram displays the function of each of the corresponding enzymes along the glycolytic and tricarboxylic acid cycle pathways. Abbreviations: Glu=glucose; P=phosphate; G=glycerate; Pyr=pyruvate; PDH=pyruvate dehydrogenase; HK=hexokinase (e) Maximum-normalized expression of 20 ribosome and translation-related transcripts regulated at the small DP to CD69$^+$ DP transition. The following genes encode the structural ribosomal proteins: Rpl3, Rpl37, Rpl38, Rpl39, Rplp1, Rps12, Rps20, Rps25, Rps28, Rps29, Rrp15, Rpsa.

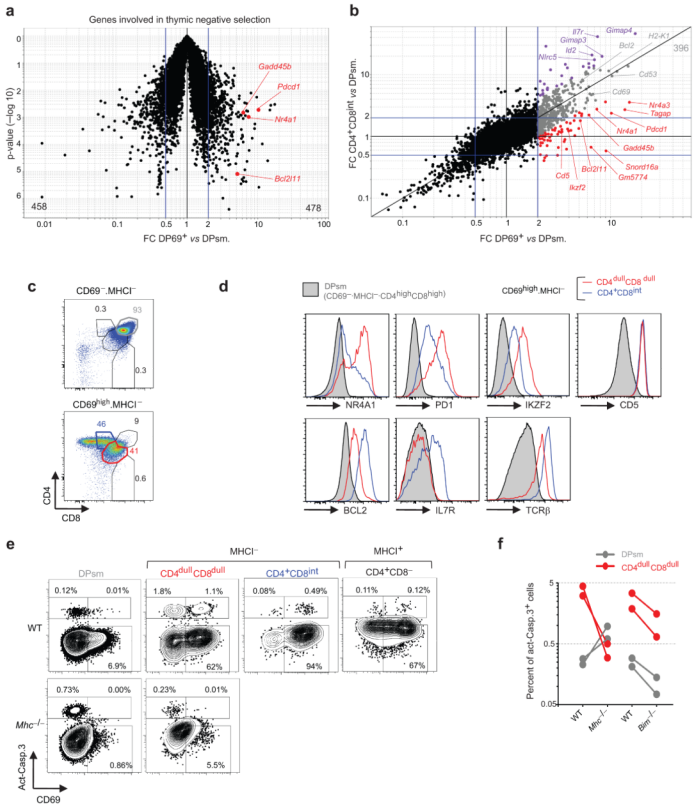

Figure 6.

Transcriptional and functional footprints of clonal deletion in CD69^{+} DP thymocytes. **(a)** Volcano plot comparing CD69^{+} DP (DP69^{+}) and small DP (DPsm) thymocytes (Fold Change: x axis; t test p-value: y axis). Genes which have been reproducibly associated with negative selection in TCR transgenic models are highlighted in red. **(b)** Fold change/FC plot showing transcriptome changes induced in CD69^{+} DP (DP69^{+}) (x-axis) and intermediate (CD4^{+}CD8^{int}) thymocytes, relative to small DP (DPsm). Blue lines mark a FC >2. Genes induced by >2-fold in CD69^{+} DP thymocytes and showing higher (violet), similar (gray), or, lower (red) upregulation in intermediate thymocytes are highlighted. **(c)** Expression of CD4 and CD8 on CD69^{neg}MHCI^{neg} (top) or CD69^{hi}MHCI^{neg} (bottom) thymocytes (see gating strategy in Supplementary Fig. 7). The frequencies of cells falling within each gate are indicated. **(d)** Cell surface expression of PD-1, IL-7R, CD5, TCRβ, and intracellular expression of IKZF2 (HELIOS), NR4A1, BCL2 on indicated subpopulations (see key). Panels (c-d) are representative of three independent experiments. **(e)** Intracellular expression of the activated, cleaved form of Caspase-3 (Act-Casp.3) and CD69 on subpopulations defined in panels (c-d), from WT and *b2m*$^{-/-}$.*Iab*$^{-/-}$ (*Mhc*$^{-/-}$) mice. **(f)** Proportion of activated Caspase-3^{+} cells within the indicated thymocyte subpopulations from *b2m*$^{-/-}$.*Iab*$^{-/-}$ (*Mhc*$^{-/-}$), *Bcl2l11*$^{-/-}$ mice (*Bim*$^{-/-}$) and wild-type (WT) mice. Each pair of mice corresponds to one experiment.

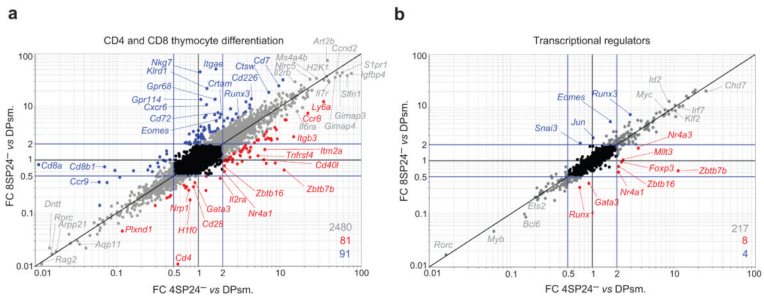

Figure 7.

Acquisition of CD4 and CD8 transcriptional identities during thymocyte differentiation**. (a)** Fold change/FC plot showing transcriptome changes induced in mature CD4SP (4SP24⁻) (x-axis) and mature CD8SP (8SP24⁻) thymocytes (y-axis), relative to small DP (DPsm). Blue lines mark a FC of 2. Genes showing similar (gray) or preferential upregulation during CD4SP (red) or CD8SP (blue) differentiation are highlighted (FC threshold of 2, with the corresponding number of genes indicated). **(b)** Same as (a), filtered using a list of 1,680 known or putative transcriptional regulators (provided in Supplementary Table 4**)**.

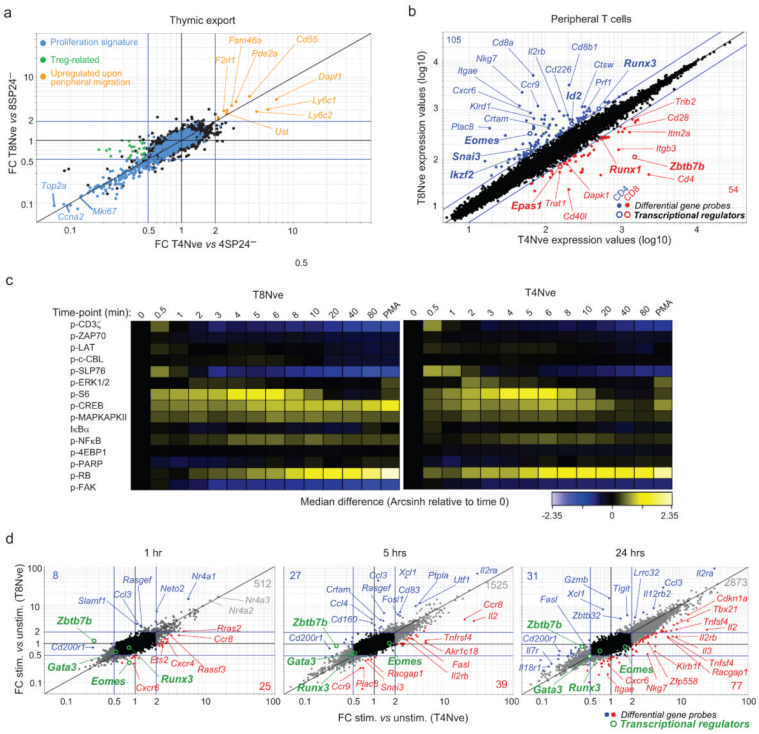

Figure 8.

Definition of CD4 and CD8 transcriptional identities. **(a)** Fold change/FC plot showing transcriptome changes induced in lymph node CD4 (x-axis) and CD8 T cells (y-axis), relative to their respective thymic parental populations, mature CD4SP (4SP24^{-}) (x-axis) and mature CD8SP (8SP24^{-}) thymocytes (y-axis). Blue lines mark a FC of 2. Genes upregulated by >2-fold in peripheral CD4 and CD8 T cells, relative to their thymic counterparts, are highlighted in orange. Treg cell-related and proliferation signature genes are highlighted in green and blue, respectively (see text). **(b)** Expression/expression plot comparing lymph node CD4 (x-axis) and CD8 T cell transcriptomes (y-axis). Genes preferentially expressed in CD4^{+} (red) or CD8^{+} (blue) T cells are highlighted, with the corresponding number of gene probes. Transcriptional regulators are indicated in bold. **(c)** Heatmaps showing the level of phosphorylation of indicated signaling molecules in CD8^{+} (left) and CD4^{+} (right) lymph node T cells, detected simultaneously by mass cytometry at multiple time points following anti-CD3 and anti-CD28 crosslinking. Cells were fixed after antibody crosslinking at the indicated time points and analyzed on the CyTOF instrument. First column, unstimulated cells; Last column, PMA positive control. Panel c is representative of 4 independent experiments. **(d)** Fold change/FC plots showing transcriptome changes induced in anti-CD3and anti-CD28 stimulated CD4^{+} (x-axis) and CD8^{+} lymph node T cells (y-axis), relative to corresponding unstimulated cell populations at the indicated time points. Blue lines mark a FC of 2. Genes showing similar (gray) or lineage preferential regulation in CD4^{+} T cells (red) or CD8^{+} T cells (blue) are highlighted (FC threshold >2, with the corresponding number of genes indicated).